Available online at www.sciencedirect.com
ScienceDirect
Applied Radiation and Isotopes 65 (2007) 313–317
Applied Radiation and Isotopes
www.elsevier.com/locate/apradiso

# Derivation of $V$ function for LR 115 SSNTD from its sensitivity to $^{220}$Rn in a diffusion chamber

S.Y.Y. Leung[a], D. Nikezic[a], J.K.C. Leung[b], K.N. Yu[a,*]

[a]*Department of Physics and Materials Science, City University of Hong Kong, Tat Chee Avenue, Kowloon Tong, Kowloon, Hong Kong*
[b]*Department of Physics, The University of Hong Kong, Pokfulam Road, Hong Kong*

Received 24 April 2006; received in revised form 12 July 2006; accepted 10 August 2006

**Abstract**

The sensitivity of the LR 115 detector inside a diffusion chamber to $^{220}$Rn gas concentration is dependent on the removed active layer thickness during chemical etching. This dependence is related to the $V$ function for the LR 115 detector (where $V$ is the ratio between the track etch velocity $V_t$ and the bulk etch velocity $V_b$) and the geometry of the diffusion chamber. The present paper presents the experimentally determined relationship between the sensitivity of the LR 115 detector inside a Karlsruhe diffusion chamber (determined from the number of etched tracks completely penetrating the active cellulose nitrate layer) and the removed active layer thickness. These data were used to derive the $V$ function for the LR 115 detector, which took the functional form of the Durrani–Green's function, i.e., $V = 1 + (a_1 e^{-a_2 R} + a_3 e^{-a_4 R})(1 - e^{-a_5 R})$, with the best-fitted constants as $a_1 = 14.50$, $a_2 = 0.50$, $a_3 = 3.9$ and $a_4 = 0.066$.


*Keywords:* Diffusion chamber; Solid-state nuclear track detector; LR 115 detector; Track etch; Bulk etch

## 1. Introduction

Track growth in solid state nuclear track detectors (SSNTDs) has been suggested to base on two parameters, $V_t$ and $V_b$, by Fleisher et al. (1975), where $V_t$ is the track etch rate (i.e., the rate of etching along the particle trajectory) and $V_b$ is the bulk etch rate (i.e., the rate of etching of the undamaged detector surface) or, equivalently, on the ratio $V = V_t/V_b$. With the $V$ function, together with a track growth model (e.g., Nikezic and Yu, 2003a), the track parameters including the lengths of the major and minor axes, can be calculated, and their profiles can be plotted (Nikezic and Yu, 2002, 2003b, 2006).

The present work explores a method to derive the $V$ function for the LR 115 SSNTD from its sensitivity to $^{220}$Rn in a diffusion chamber (determined from the number of etched tracks completely penetrating the active cellulose nitrate layer). The use of diffusion chamber is one of the standard methods for long-term measurements of $^{222}$Rn concentrations. In this method, a piece SSNTD, the most commonly used being the LR 115 and CR-39 SSNTDs, is placed inside a diffusion chamber. Being a gas, $^{222}$Rn can diffuse into the diffusion chamber. The $^{222}$Rn gas, together with the progeny formed from $^{222}$Rn decay, inside the diffusion chamber can irradiate the SSNTD and leave behind latent tracks. On chemical etching, the tracks can be visualized and can be counted under an optical microscope with suitable magnification. The technique of using diffusion chamber has been widely used and described in the literature (Khan et al., 1993; Durrani and Ilic, 1997; Nikolaev and Ilic, 1999), and a recent review on the SSNTDs has been given by Nikezic and Yu (2004). In the present work, the SSNTD studied will be the LR 115 detector (from DOSIRAD, France).

In applying the diffusion chamber method, the track density (number of tracks per unit area) per unit time on the LR 115 SSNTD is measured, which has the unit of [$m^{-2}\,s^{-1}$]. The average $^{222}$Rn or $^{220}$Rn gas concentration (in [$Bqm^{-3}$]) during the exposure period is obtained by dividing the track density per unit time with the sensitivity (in [m]). However, different track densities, and thus

*Corresponding author. Tel.: +852 27887812; fax: +852 27887830.
*E-mail address:* peter.yu@cityu.edu.hk (K.N. Yu).

0969-8043/$ - see front matter © 2006 Elsevier Ltd. All rights reserved.
doi:10.1016/j.apradiso.2006.08.006

different sensitivities, will be obtained for different removed active layer thickness of the LR 115 SSNTDs. The dependence is related to the $V$ function for the LR 115 detector, the geometry of the diffusion chamber and, in the case of $^{222}$Rn, the deposition fraction of $^{218}$Po in the diffusion chamber (Koo et al., 2003). Therefore, the sensitivities would also provide very useful information for examination of the $V$ function.

For the case of $^{222}$Rn, after $^{222}$Rn diffuses into the diffusion chamber, $^{218}$Po will be formed. A fraction $f$ of $^{218}$Po decays before deposition onto available inner surfaces of the chamber. Therefore, the use of sensitivities to $^{222}$Rn in the diffusion chamber will inevitably have the additional uncertainty from $f$ although we have previously determined $f$ to be ~0.4, which seems to be independent of the shape and dimensions of the diffusion chambers, the surface to volume ratios or the internal surface materials of the diffusion chambers (Koo et al., 2002, 2003). In order to avoid the possible uncertainties introduced by $f$, we will focus on using the sensitivities to $^{220}$Rn in the present work.

The first task of the present study is to experimentally determine the sensitivities of the LR 115 SSNTD to $^{220}$Rn in a diffusion chamber for different removed active layer thickness. From these data, the $V$ function for the LR 115 detector will be derived.

## 2. Experimental methodology

The diffusion chambers employed for the present study were conical, with the inner base radius of 2.35 cm, top radius of 3.35 cm and height of 4.8 cm, and are commonly referred to as the "Karlsruhe" diffusion chambers. There were holes in the brim of chamber, which allow air to flow in and out of the chamber (see Fig. 1). This type of diffusion chamber has been used for routine measurements of $^{222}$Rn or $^{220}$Rn concentrations.

The LR 115 detectors (Type 2, non-strippable) were purchased from DOSIRAD, France. The LR 115 detector consists of a 12 μm red cellulose nitrate active layer and 100 μm clear polyester base substrate as declared by the manufacturer. A piece of 3 cm × 3 cm LR 115 detector was placed on the bottom of the diffusion chamber and a filter paper across the top to prevent $^{222}$Rn/$^{220}$Rn progeny from getting insider the diffusion chamber.

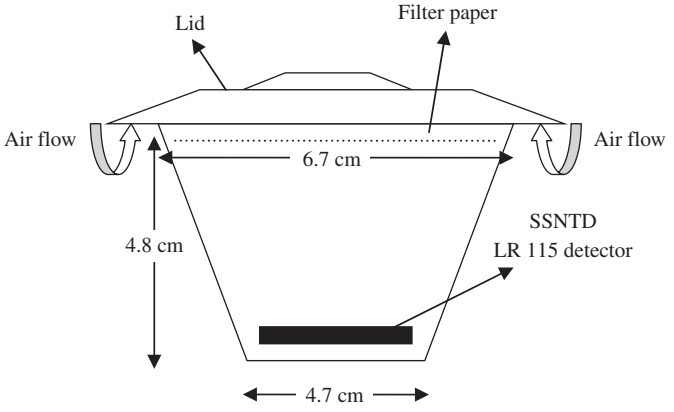


Fig. 1. The dimensions of the Karlsruhe diffusion chamber used in the present investigation with a top radius of 3.35 cm, inner base radius of 2.35 cm and height of 4.8 cm. The SSNTD and the filter paper were placed on the bottom and across the top of the diffusion chamber, respectively.

The diffusion chambers with the SSNTDs were inserted into the $^{220}$Rn exposure chamber (Leung et al., 1994) through an air lock. The experimental set-up for the exposures is shown in Fig. 2. The exposures were carried out in a re-circulating mode for 3-d. The $^{220}$Rn gas concentrations inside the exposure chamber were monitored by RAD-7 (Durridge Company Inc., MA) with a sampling period of 30 min. A total of 5 separate exposures were used, with the average $^{220}$Rn concentrations from 830 to 1050 Bqm$^{-3}$, which gave altogether 14 samples.

After the 3-d exposures, the SSNTDs were removed from the diffusion chambers for chemical etching in 10% aqueous NaOH at 60 °C for approximately 1 h. The temperature was kept constant with an accuracy of ±1 °C. The detectors were etched using a magnetic stirrer (Model no: SP72220-26, Barnstead/Thermolyne, Iowa, USA) so as to provide more uniform etching (Yip et al., 2003a). After etching, the detectors were taken out of the etchant, rinsed with de-ionized water and dried.

For the LR 115 SSNTD, it has been found that the removed active layer during chemical etching is significantly affected by the presence and amount of stirring, and thus cannot be controlled easily (Yip et al., 2003a). Different methods have been used to measure the active layer thickness of LR 115 detectors, e.g., surface profilometry (Nikezic and Janicijevic, 2002; Yip et al., 2003a), absorption of X-ray fluorescence photons (Yip et al., 2003b), infrared absorption (Ng et al., 2004) and gray level determination (Yu and Ng, 2004). The infrared absorption method (Ng et al., 2004) is adopted in the present work. The active layer thickness of the detector was obtained through the infrared absorption determined using a Perkin-Elmer Fourier transform infrared (FTIR) spectroscopy system (Model 16 PC FT-IR) for 10 cycles. The scanned diameter was 9 mm so the scanned area was 0.64 cm$^2$. The exponential decay relationship between the infrared transmittance at the wave number at 1598 cm$^{-1}$ (corresponding to the O–$NO_2$ bond in the cellulose nitrate) and the

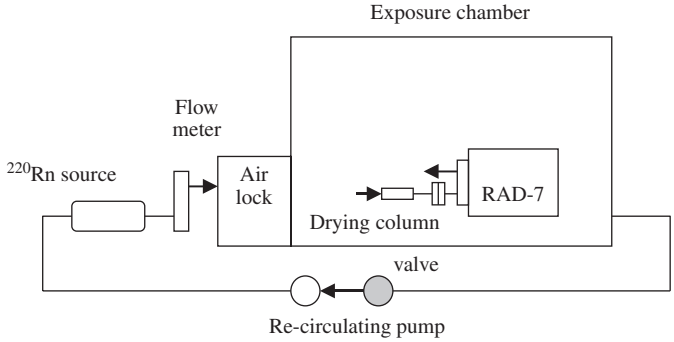


Fig. 2. The experimental set-up for the $^{220}$Rn exposure chamber.

thickness of the active layer (Ng et al., 2004) was used for the present study. For each detector, the IR transmittance values were measured at six different locations to give the average values.

The alpha-particle tracks registered by the detector were then counted under an optical microscope with 200× magnification and only those completely perforated the active layers of the LR 115 SSNTDs were counted. Knowing the time of exposure and with the $^{220}$Rn concentrations given by RAD-7, the sensitivities corresponding to different removed active-layer thickness were determined.

## 3. Results

As mentioned before, a total of 5 separate exposures were used to give a total of 14 exposed LR 115 detectors. The experimental results for the sensitivities of the LR 115 detector inside the Karlsruhe diffusion chamber to $^{220}$Rn for various removed active-layer thickness are shown in Fig. 3. It is interesting to note that the data collected from the 5 separate exposures closely follow the same trend.

Modeling the source in this problem needs two computer programs. The first one follows the history of alpha particles emitted by $^{220}$Rn and $^{216}$Po, which decay exclusively in the air volume inside the diffusion chamber. The second one follows the particles emitted from other alpha-particle emitters in the $^{220}$Rn chain ($^{212}$Bi and $^{212}$Po), which have completely deposited onto the internal walls of the diffusion chamber. Both programs have the common module which decides whether an emitted alpha particle can be detected by the LR 115 detector.

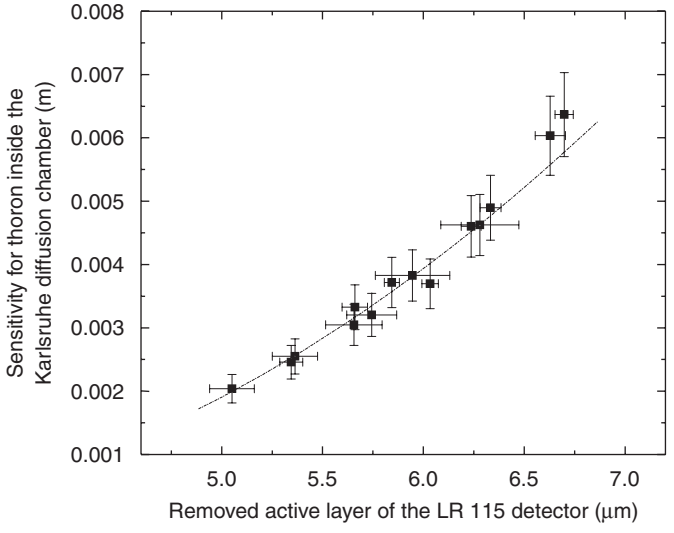


Fig. 3. The experimental data (solid squares) for the sensitivity of $^{220}$Rn inside the diffusion chamber for different removed active layer thickness and the computer simulated results obtained from the simulated $V$ function (with constants $a_1 = 14.50$, $a_2 = 0.50$, $a_3 = 3.9$ and $a_4 = 0.066$).

Monte Carlo simulations of alpha-particle propagation in air and in the LR 115 detector are performed in both cases. The simulations involve the following steps:

(1) sampling of a random emission point in the chamber volume or on the chamber wall, and the counter for *emitted* alpha particles is then increased by 1;
(2) sampling of a random direction in which the alpha particle is emitted;
(3) determining whether this particle hits the detector, based on geometrical conditions and the known range of the alpha particle in air (depending on the initial energy of the alpha particle);
(4) if the alpha particle misses the detector, generating a new particle and repeating the steps from step (1);
(5) if the alpha particle hits the detector, determining whether it will be detected or not. If "yes", the counter for *detected* alpha particles is increased by 1. If "no", generating a new particle and repeating the steps from step (1).

Steps (1)–(5) are repeated a large number of times to minimize the statistical uncertainty. When the number of detected particles reaches the pre-determined number (which is $10^5$ in our case), the simulations are terminated and the detection efficiency is then calculated as the ratio between the numbers of *detected* and *emitted* alpha particles. The sensitivities for the chamber volume and the chamber wall are summed up to obtain the final sensitivity.

Our track growth model (Nikezic and Yu, 2003a) was employed for the calculations. Input parameters in the model included the $V$ function and the removed active layer during chemical etching. The incident energies of alpha-particles from $^{220}$Rn and its progeny on the LR 115 SSNTD were used to calculate the ranges of the corresponding alpha particles in the detector material, which were accomplished using the SRIM program (Ziegler, 2001) by assuming that the LR 115 detector was based on cellulose nitrate (with the chemical composition $C_6H_8O_9N_2$ and a density $\rho = 1.4\,\mathrm{g\,cm^{-3}}$).

The $V$ function published by Durrani and Green (1984) was adopted in the present investigation in a modified form. The form of this function is

$$V = \frac{V_t}{V_b} = 1 + (a_1 e^{-a_2 R} + a_3 e^{-a_4 R})(1 - e^{-a_5 R}), \quad (1)$$

where $R$ is the residual range of the alpha particles. The constants $a_1$, $a_2$, $a_3$, $a_4$ and $a_5$ for the function in Eq. (1) were given by Durrani and Green (1984) as 100, 0.446, 4, 0.044 and 1, respectively, and by Durrani and Bull (1987) as 100, 0.446, 5, 0.107 and 1, respectively.

We systematically adjusted the constants $a_k$, where $k = 1$ to 4, while keeping $a_5 = 1$, in order to obtaining the best agreement with our 14 experimental data points through

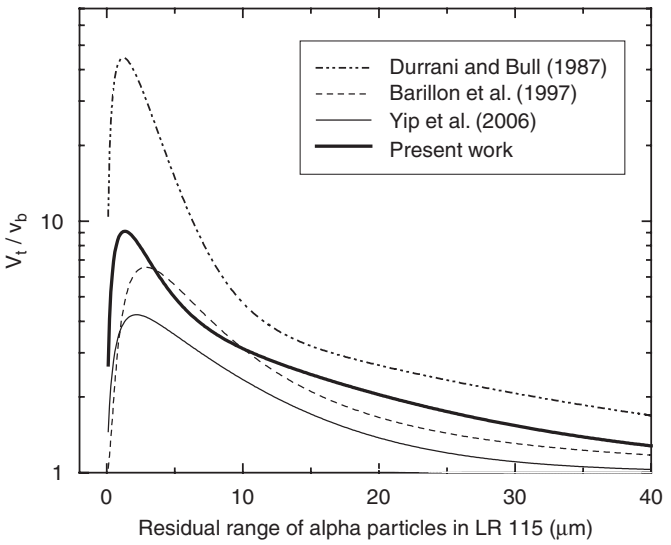


Fig. 4. The $V$ function derived from the sensitivity to $^{220}$Rn inside the diffusion chamber (present work) and three other previously derived $V$ functions.

minimization of $N$ defined as

$$N = \sum_{j=1}^{14} \sqrt{[\eta_{exp}(j) - \eta_{calc}(j)]^2}, \quad (2)$$

where $\eta_{exp}$ and $\eta_{calc}$ are the sensitivities to $^{220}$Rn inside the diffusion chamber obtained from experiment and simulation, respectively.

The constant $a_1$ was changed from 10 to 30, with steps of 10; $a_2$ from 0.3 to 0.5 with steps 0.1; $a_3$ from 4 to 6 with steps 1, and $a_4$ from 0.06 to 0.08 with steps 0.005. When the constants $a_k$ are varied, $N$ showed some oscillatory behavior. When the first run with the ranges and steps given above was finished and the best combination (where $N$ was smallest) was found, the second run was performed varying the constants about the best values obtained in the first run, with much smaller steps. This procedure was repeated several times in order to find the combination of constants that gave the smallest $N$. In this way we found the best combination of constants as $a_1 = 14.50$, $a_2 = 0.50$, $a_3 = 3.9$ and $a_4 = 0.066$. Our $V$ function is then obtained by substituting these constants into Eq. (1), which is shown in Fig. 4.

The simulated sensitivities of the LR 115 SSNTD to $^{220}$Rn inside the diffusion chamber using the simulated $V$ function have also been plotted in Fig. 3 for comparison with the experimental results. It can be seen that the simulated sensitivities reproduce the experimental results very satisfactorily.

## 4. Discussion

The function from Durrani and Green (1984) given in Eq. (1) with the constants given by Durrani and Bull (1987) is shown in Fig. 4. A maximum appears close to the end of the particle range, which corresponds to the Bragg peak in the stopping power curve. The maximum is very high, with $V_{max} \approx 45$. A nominal $V_b \approx 3.3\,\mu m\,h^{-1}$ (Nikezic and Janicijevic, 2002) will give $V_t \approx 150\,\mu m\,h^{-1}$, which may be too high. For example, according to SRIM, the range of alpha particles with energy of 2.5 MeV is 11.8 μm. By evaluating $\int_0^{11.8} dx/V_t(R'-x)$, one may show that such tracks take only about 28 min of etching to perforate the sensitive layer. Another 20 min of etching will be needed to obtain visible tracks when the bottom of the tracks achieves the diameter in the order of 1 μm. Therefore, the total time needed to obtain visible tracks is about 50 min, which is only half the time elapsed when the first track appears according to Barillon et al. (1997).

Barillon et al. (1997) also published a $V$ function for alpha-particle tracks in LR 115 in the form

$$V_t = V_b + \frac{1}{a_1^2 + [a_2 R - (1/a_3 R)]^2} \quad (3)$$

with constants $a_1 = 0.23$, $a_2 = 0.032$ and $a_3 = 3.8$. In the same paper, they also tried a $V_t$ function which was proportional to the ionizing rate $I$, i.e., $V_t = KI$, where $K$ was a proportionality constant, and they concluded that this approach was unsuccessful because of the lack of information between the process of physical energy loss and creation of damages in the detector material that were responsible for the etching process. The function in Eq. (3) is also shown in Fig. 4.

Yip et al. (2006) also determined the $V$ function for alpha-particle tracks in LR 115 in the form of the function of Durrani and Green (1984). They systematically irradiated LR 115 SSNTDs with alpha particles in the energy range from 1 to 5 MeV with incident angles from 30° to 90°. After chemical etching to remove a thickness of about 6.5 μm, the lengths of the major and minor axes of the alpha-particle track openings in the films were measured with an image analyzer. These data were used altogether to obtain the constants as $a_1 = 2.14$, $a_2 = 0.12$, $a_3 = 2.7$ and $a_4 = 0.135$ ($a_5 = 1$). This function is also shown in Fig. 4 for a comparison.

From Fig. 4, we can see that the function of Durrani and Bull (1987) is very different from other three functions presented here, while these three functions are relatively commensurate among one another although there are some discrepancies. The maximums of the functions of Durrani and Bull (1987), Barillon et al. (1997), Yip et al. (2006) and the present work are about 45, 6.5, 4 and 9, respectively. In the region of larger residual ranges, i.e., above 20 μm, all the functions, and in particular the last three functions, converge to values close to 1.

The discrepancies between the function derived in the present work and that of Yip et al. (2006) are worth particular mentioning, since the SSNTDs and the etching conditions have been the same in these two studies. The present study was based on the track density while that of Yip et al. (2006) was based on the track opening dimensions. Whether these differences in methodologies, or the uncertainties involved in these methodologies, have

led to the observed discrepancies is still unclear. A more detailed investigation on these discrepancies will be carried out in a future study.

## Acknowledgment

The present research is supported by the Strategic Research Grant 7001829 from the City University of Hong Kong.

## References

Barillon, R., Fromm, M., Chambaudet, A., Marah, H., Sabir, A., 1997. Track etch velocity study in a radon detector (LR 115, cellulose nitrate). Radiat. Meas. 28, 619–628.

Durrani, S.A., Bull, R.K., 1987. Solid State Nuclear Track Detection. Principles, Method and Applications. Pergamon Press, Oxford.

Durrani, S.A., Green, P.F., 1984. The effect of etching conditions on the response of LR 115. Nucl. Tracks 8, 21–24.

Durrani, S.A., Ilic, R., 1997. Radon measurements by etched track detectors. Applications in Radiation Protection, Earth Sciences and the Environments. World Scientific, Singapore.

Fleisher, R.L., Price, P.B., Walker, R.M., 1975. Nuclear Track in Solids. Principles and Applications. University of California Press, Berkley.

Khan, H.A., Qureshi, I.E., Tufail, M., 1993. Passive dosimetry of radon and its daughters using solid state nuclear track detectors (SSNTDs). Radiat. Prot. Dosim. 46, 149–170.

Koo, V.S.Y., Yip, C.W.Y., Ho, J.P.Y., Nikezic, D., Yu, K.N., 2002. Experimental study of track density distribution on LR 115 detector and deposition fraction of $^{218}$Po in diffusion chamber. Nucl. Instr. Meth. Phys. Res. A. 491, 470–473.

Koo, V.S.Y., Yip, C.W.Y., Ho, J.P.Y., Nikezic, D., Yu, K.N., 2003. Deposition fractions of $^{218}$Po in diffusion chambers. Appl. Radiat. Isot. 59, 49–52.

Leung, J.K.C., Jia, D., Tso, M.Y.W., 1994. A fully automated radon exposure chamber. Nucl. Instr. Meth. Phys. Res. A. 350, 566–571.

Ng, F.M.F., Yip, C.W.Y., Ho, J.P.Y., Nikezic, D., Yu, K.N., 2004. Non-destructive measurement of active-layer thickness of LR 115 SSNTD. Radiat. Meas. 38, 1–3.

Nikezic, D., Janicijevic, A., 2002. Bulk etching rate of LR 115 detector. Appl. Radiat. Isotop. 57, 275–278.

Nikezic, D., Yu, K.N., 2002. Profiles and parameters of tracks in the LR115 detector irradiated with alpha particles. Nucl. Instr. Meth. B 196, 105–112.

Nikezic, D., Yu, K.N., 2003a. Three-dimensional analytical determination of the track parameters: over-etched tracks. Radiat. Meas. 37, 39–45.

Nikezic, D., Yu, K.N., 2003b. Calculations of track parameters and plots of track openings and wall profiles in CR39 detector. Radiat. Meas. 37, 595–601.

Nikezic, D., Yu, K.N., 2004. Formation and growth of tracks in nuclear track materials. Mater. Sci. Eng. R 46, 51–123.

Nikezic, D., Yu, K.N., 2006. Computer program TRACK_TEST for calculating parameters and plotting profiles for etch pits in nuclear track materials. Comput. Phys. Commun. 174, 160–165.

Nikolaev, V.A., Ilic, R., 1999. Etched track radiometers in radon measurements: a review. Radiat. Meas. 30, 1–13.

Yip, C.W.Y., Ho, J.P.Y., Koo, V.S.Y., Nikezic, D., Yu, K.N., 2003a. Effects of stirring on the bulk etch rate of LR 115 detector. Radiat. Meas. 37, 197–200.

Yip, C.W.Y., Ho, J.P.Y., Nikezic, D., Yu, K.N., 2003b. A fast method to measure the thickness of removed layer from etching of SSNTD based on EDXRF. Radiat. Meas. 36, 161–164.

Yip, C.W.Y., Nikezic, D., Ho, J.P.Y., Yu, K.N., 2006. Chemical etching characteristics for cellulose nitrate. Mater. Chem. Phys. 95, 307–312.

Yu, K.N., Ng, F.M.F., 2004. Fast and non-destructive determination of active-layer thickness of LR 115 SSNTD using a color commercial document scanner. Nucl. Instr. Meth. Phys. Res. B. 226, 365–368.

Ziegler, J.F., 2001. SRIM-2000, 〈http://www.srim.org/〉.